Research Article

Signal convolution indicates chromatographic pulse flow and open-end flow

Jens E. T. Andersen[1] · Hawa W. Mukami[1] · Irene W. Maina[1]

Abstract
Only slices are measured of very long segments of solute molecules that are injected into columns in chromatographic systems. Since the concentration of solute molecules changes during elution as a function of time, the observed signal should be re-constructed for a comparison of experimental results with theory. The influence of response time on the observed signal in high-performance liquid chromatography experiments was investigated in detail using a C-18 column for the measurement of caffeine in pure methanol as eluent. The response function influenced the observed signal by converting the square signal of pulse flow into a chromatographic peak. At faster linear flow rates (LFRs), the response function influenced the observed shape of the chromatographic peak, whereas diffusion dominated at slow LFRs. By convolution of the square signal with the response function, it was possible to predict the shape of the observed signal and chromatographic parameters and to provide an alternative explanation to the van Deemter equation. By using the shape of a known response function and modelling the new theory to data, it was proposed that the injected solute molecules were eluted over long distances through the chromatographic column, distances that are much longer than the physical length of the system.

Keywords Physical fluid dynamics · Pulse flow · Chromatography · van Deemter equation · Convolution

Mathematics Subject Classification 76A02

JEL Classification C20 · C22 · C29

1 Introduction

Separation by chromatography and identification of chemical species by various types of analytical technologies are key in analytical chemistry activities [1]. Recent developments in chromatography include analysis of chiral compounds [2], high-speed analysis [3–5], microanalysis [6–8], nano analysis [9] and lab-on-a chip [10]. The optimization and understanding of chromatographic systems rely on two theories or combinations thereof: adsorption theory [11, 12] and plate theory [13, 14]. The retention and separation of chemical species is understood in terms of adsorption and partitioning [13]. Although the mechanisms are different, both theories are important in describing and understanding the chromatographic phenomenon [15]. The injection of small volumes of chemical species into a pipe with transport media such as gases [5, 16], liquids [15] or mixtures of gases and liquids [17] produces peaks of similar shapes, as observed by appropriate detection units [18]. Chromatographic peaks even resemble those of flow through pipes without chromatographic columns where injected volumes do not undergo separations [19, 20]. Longitudinal diffusion and laminar flow characterize flow through pipes [19, 21], but such concepts

✉ Jens E. T. Andersen, andersenj@biust.ac.bw | [1]Department of Chemical and Forensic Sciences, Botswana International University of Science and Technology, Plot 10071, Boseja Ward, Private Bag 016, Palapye, Botswana.

SN Applied Sciences (2019) 1:1221 | https://doi.org/10.1007/s42452-019-1271-0

Received: 10 May 2019 / Accepted: 12 September 2019 / Published online: 16 September 2019

were not treated earlier in relation to flow through chromatographic columns.

The retention mechanisms of gas chromatography produce Gaussian-shaped distributions by the longitudinal diffusion of solute molecules that move over distances of 30–60 m through coiled open-tube columns [16, 22, 23]. Significant tailing and peak skewness are observed for most types of chromatographic peaks, which is attributed to column overload or inhomogeneities of the column [24]. Peak broadening [25] originates from several contributions comprising longitudinal diffusion, eddy diffusion, mobile-phase mass transfer, stagnant-mobile-phase mass transfer and stationary-phase mass transfer [26]. The efficacy of peak separation and retention depends on the column length, temperature [27], particle size of the stationary phase, porosity of the column material [14, 28], column packing [29, 30], flow rate [7], diffusion rate and, to a large extent, composition of the mobile phase [31]. In high-performance liquid chromatography (HPLC), changing the solvent composition of the mobile phase corresponds to an adjustment of the hydrophobic and hydrophilic interactions among the solute, mobile phase and stationary phase [31, 32].

Laminar flow prevails at low Reynolds numbers less than approx. 2500 [33], which defines the limit for transition into turbulent flow. However, turbulent flow may be observed at Reynolds numbers much lower than 2500, even as low as 1–10, when retention is induced by chromatographic columns [34]. Most chromatographic theories predict a Gaussian-shaped distribution of concentrations along the length of the pipe [13, 14], and the corresponding full width at half maximum (FWHM) increases as a function of time when the segment moves downstream. The optimum conditions of peak shape with respect to chromatographic separation are described by the Van Deemter equation [23], which is widely used for purposes of optimization [35]. Very large injection volumes produce long segments when injected into narrow pipes, and the resulting 'square distribution' of the concentration of solute molecules is pulse-like [11, 25, 36] rather than Gaussian shaped [11, 37]. The chromatographic peak is observed not as a square signal, but as a signal that is smoothed by the response function of the detector, extra-column band broadening [38, 39] and column-only band broadening [40]. Correction for extra-column band broadening was performed by Wright et al. [36] who used a digital system peak with a tail and the Dirac-delta function to perform the deconvolution of the peak. That correction provided peaks with no tail and slightly reduced retention times, and it added to the understanding of plate theory [36]. Vanderheyden et al. [35] introduced peak deconvolution by using the Pap–Pápai equation [41] and two exponentially-modified Gaussian curves to describe the peak. After significant corrections for noise phenomena, was obtained by means of peak-width methods and moment methods excellent correspondence between theory and experiment, also in strong support to plate theory [35]. Deconvolution by means of Fourier transforms results in drawbacks with reduction of noise that need be dealt with according to additional empirical theories [35, 36]. The lag time of the detector has a smoothing effect on the observed signal [38], and the degree of influence on the signal of chromatographic elution is investigated herein for the simple case of pulse flow. The time constant of the detector is more important in shaping the observed signal than the sampling rate of the system is. Significant peak tailing is observed when the time constant of the detector increases [38], and the present investigation focuses entirely on this effect and features of laminar flow [19], which is used to provide alternative explanations for the chromatographic features. Thus, a square function was applied rather than a step function [38], and both rise time and fall time were included in the description.

The principle of peak deconvolution by Gaussian functions is a widely accepted method of extracting additional information about the constituents of the observed peak [35, 36, 42]. In chromatography, deconvolution has two different meanings comprising: (1) To prepare a linear combination of Gaussian functions to describe the observed peak [42], (2) Perform signal reconstitution by mathematical deconvolution of the observed peak with an extra-column band broadening function [35, 36]. However, convolution and deconvolution by the apparatus' response function may be used to describe phenomena of flow through pipes and chromatography [43, 44], which in most experimental setups provide peak shapes that cannot be compared directly to theoretical calculations; convolution or deconvolution should be applied to the analysis. Most frequently, chromatographic detection cells are very short in comparison to the length of segments of chemicals that are injected into the narrow-bore pipes. Thus, events within the pipe are monitored in a slice-like manner in the short detection cell whilst the injected pulse simultaneously changes shape during measurement.

By assuming that the underlying mechanisms of all types of pipe flow are the same, based upon the similarity of peak shapes and van Deemter behaviour [23, 45], it was proposed here that the distribution of molecules within square-pulse segments during flow through pipes may be characterized by the detector's response function rather than by using a Gaussian-shaped function of diffusion. The Gaussian-shaped distribution of molecules [19, 22, 23] was contested [12], and it was the aim to provide an alternative understanding of pipe flow through columns by introducing procedures of time-based convolution. It was indicated that solute molecules in the injected pulse-shaped

concentration distribution travelled long distances, and this result unifies the description of open-end pipe flow and fluid and gas flow through chromatographic columns. This understanding of the chromatography experiment provided simplified equations to describing peak shape, retention time, band broadening, peak asymmetry, the van Deemter equation and total area of the peak.

2 Experimental

2.1 Materials

High-performance liquid chromatography (HPLC)-grade methanol (CAS Registry Number: 67-56-1, Merck) and caffeine (CAS Registry Number: 58-08-2, Sigma-Aldrich) working standards were of analytical grade. They were used without further purification.

2.2 Instrumentation

The HPLC 1260 Infinity system consisted of an Infinity quaternary pump, high-performance degasser module, diode array detector (DAD) (254 nm) and Infinity auto sampler. Data were recorded at 20 Hz with a response time of 0.2 s and processed by Chem-station software (Agilent Technologies, California, USA). The chromatographic separations were performed by a C-18 Phenomenex column (150 mm × 4.5 mm i.d., particle size 5 µm) under isocratic conditions.

2.3 Chromatographic conditions

The mobile phase consisted of 100% methanol, which was used as the eluent in isocratic mode, and the response of caffeine was monitored at a detection wavelength of 254 nm. The mobile phase was filtered through a 0.45 µm membrane filter and degassed before use. The injection volume was 20 µL, and all analyses were performed with the column temperature held at 30 °C; the maximum time of elution was 120 min. The flow rate and concentration of caffeine were chosen to obtain acceptable responses within the linear range of response (250 mg dm^{-3}). A total of 21 peaks (Fig. 1) with linear flow rates (LFRs) ranging between 0.0073 and 3.7 m s^{-1}, which are equivalent to 0.01 mL min^{-1} and 5.0 mL min^{-1}, respectively, were applied in the investigation. Two independent series of measurements were conducted subsequent to conditioning the chromatographic column. It should be noted, however, that results with up to 20% deviation with respect to peak absorbance were obtained during conditioning of the column. Therefore, the present experiments address the precision and assessment of parameters, but conditions

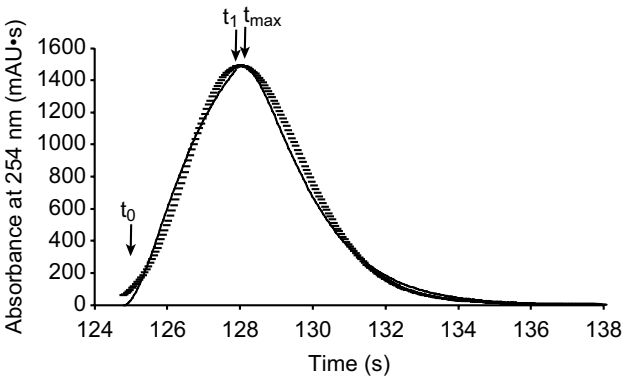

Fig. 1 Fitting of theory to experimental data at a linear flow rate of 0.37 m s^{-1} (~0.5 mL min^{-1}) (–). Full line from t_0 to t_1: calculated signal whilst the travelling pulse of solute was present within the detection cell (Eq. 2a). Full line from t_1: calculated signal (Eq. 2b) after the pulse has left the detection cell. The peak maximum (Eq. 3) was found at a time slightly delayed with respect to t_1 owing to the lag time and memory effect of the detector

of trueness and accuracy would require additional experiments and statistical analysis. The overall level of uncertainty was comparable with that in earlier investigations [46].

3 Results and discussion

3.1 Time-based convolution

When a detector signal rises and decays exponentially and simultaneously, the corresponding response function, *R(t)* of the maximum response (α) in units of AU and decay parameter (β) in units of s^{-1} may be described by the following Eq. (1) [43, 47]:

$$R(t) = \alpha \cdot exp[\beta \cdot t] \cdot (1 - exp[\beta \cdot t]) \quad (1)$$

By experiments in the present investigation, the parameters were determined to be $\alpha = (8750 \pm 610)$ mAU and $\beta = (-3.39 \pm 0.38)$ s^{-1}, where the reciprocal value of β is the characteristic response time of the detector, $t_D = -\frac{1}{\beta} = (0.295 \pm 0.033)$s, which corresponds to the manufacturer's response time of 0.2 s at a 20 Hz sampling rate. Hence, the corresponding rise time [36] to reach 90% of the maximum response would be approx. 0.44 s.

Upon injection and until the front of the pulse reaches the detector, the signal $y(t < t_0)$ is zero. Convolution with respect to time (Eq. 1) of the pulse passing the detection cell provides the following set of equations [43]:

$$y_1(t) = \frac{H \cdot L_c}{2} \cdot (p-1)^2 \quad t_0 < t < t_1 \quad (2a)$$

$$y_2(t) = y_1(t) - \frac{H \cdot L_c}{2} \cdot (q-1)^2 \quad t_1 < t \tag{2b}$$

$$p = exp\left[v_x \cdot \frac{t_0 - t}{L_c}\right] \quad L_c > 0 \tag{2c}$$

$$q = exp\left[v_x \cdot \frac{t_1 - t}{L_c}\right] \quad L_c > 0 \tag{2d}$$

where $-\alpha/\beta = \frac{H \cdot L_c}{2}$ has units of AU·s ("Appendix 1"). Equations 2a–2d describe the observed signal as separated into two fragments $y_1(t)$ and $y_2(t)$ according to the entrance time 't_0' into the detector and exit time from the detector 't_1'. The pulse flowed at a constant linear flow rate, LFR (v_x), and at slower flow rates ($v_x < 1$ m s^{-1}), the observed experimental peak was characterized by a height of $H = (6900 \pm 480)$ mAU m^{-1} s and characteristic length of $L_c = (0.555 \pm 0.011)$ m. Thus, merely four parameters (t_0, t_1, H, and L_c, Eqs. 2a–2d) were required to describe the shape of 21 chromatographic peaks. The correspondence between theory and experiment is illustrated in Fig. 1, where t_0 and t_1 are indicated with the time of maximum response (t_{max}). Owing to the exponential functions (Eqs. 2c–2d), the theoretical peak shapes are very sensitive to the choices of the time values t_0 and t_1, down to almost one hundredth of a second at fast LFRs.

Owing to the influence of the response function (Eq. 1), the time of peak maximum is slightly delayed in relation to the pulse leaving the detection cell (Fig. 1), according to the expression of Eq. 3, which represents the time of peak maximum of Eq. 2b:

$$t_{max} = t_R = t_1 + \frac{L_c}{v_x} \cdot ln\left(1 + exp\left[v_x \cdot \frac{(t_0 - t_1)}{L_c}\right]\right) \tag{3}$$

This time of response maximum (Eq. 3) is equal to the retention time (t_R) of the chromatographic peak, which may be well approximated by t_1 ($t_{max} \cong t_1$), especially at fast LFRs, where Eq. 3 reduces to Eq. 4:

$$t_R \cong t_1 \cong \frac{x_0 + L_0}{v_x} \tag{4}$$

where x_0 is the distance from the point of injection to the point of detection and L_0 is the length of the pulse. Equations 3 and 4 indicate a minor influence of the detector's response time on retention time, in accordance with earlier findings [36, 38] where it was shown that deconvolution resulted in slightly shorter retention times [36]. The reduction of retention time may then be used to provide an estimate of the value of L_c, according to Eq. 3. Injection of 20 µL of caffeine solution provided a pulse length of $L_0 = 0.88$ m within the tubular system with an inner diameter of 0.17 mm. Accordingly, the pulse was longer than the characteristic length, which indicates that solute molecules may be adsorbed by the column material and fed back into the travelling pulse at slow or moderately fast LFRs. Although the distance was expected to be approx. 1.5 m, which is the physical distance from injection to detection, a length of 45.8 ± 1.2 m was determined by multiplying t_0 with v_x. This very long travel distance may seem unlikely, but it is explained as a process by which the pulse follows unpredictable pathways through the chromatographic column (Fig. 2); this process is indicated by multiple pathways of the van Deemter model [23, 45]. A similar simplified time of entrance to the detector would indicate $t_0 \cong \frac{x_0}{v_x}$, which is valid at intermediate LFRs only.

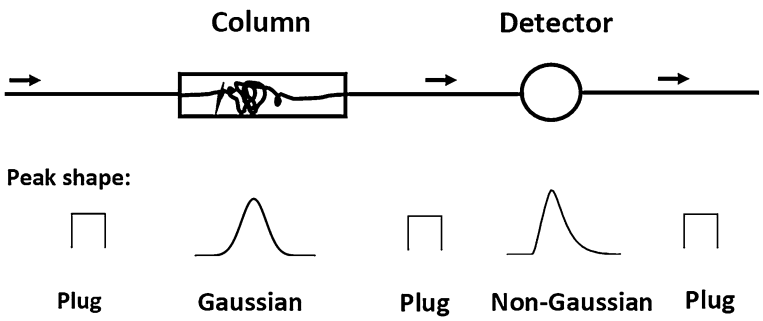

Fig. 2 Illustration of the model understanding of chromatography at intermediate LFRs. A small volume of molecules is injected into the eluent and the concentration profile is square, representing the shape of a pulse. It is proposed that the pulse-like shape is maintained whilst the volume of chemicals travels (arrows) through the column in void volumes that are created by particles of the column material. As its net movement is downstream, the pulse may also move upstream or radially to form a Gaussian-shaped 'band' of molecules within the column. The shape of the injected pulse remains unchanged as it leaves the column and moves towards the detector, where it is registered as a non-symmetric peak owing to the slow response time of the detector

3.2 Pipe flow and chromatography

In the simplified pulse model of the present investigation, all peaks were not perfectly modelled by Eqs. 2a–2d at the very front base (foot) of the peak (Fig. 1, left-hand side of peak), which indicates that the front of the pulse arrived earlier (by approx. 5%) than predicted by $t_0 \cong \frac{x_0}{v_x}$. Further, this indicates that diffusion occurs predominantly in the downstream direction. Consequently, the front of the pulse moved faster than expected, whereas the time at which the pulse exited from the detector corresponded exactly to the retention time of Eq. 4.

At LFRs faster than 1 m s^{-1}, the pulse passed through the detection cell at a time interval that approached the characteristic time of the detector (t_D, see above), $t_D \cong t_1 - t_0$. Owing to the back pressure of the column, it was not possible to exceed LFRs of $v_x = 3.7$ m s^{-1}, but even at such fast LFRs, some features of the chromatographic peak may be not visible because they travel too fast to be properly registered by the detector; this feature is known as undersampling [39]. If it were possible to obtain much faster LFRs, as in, e.g., ultra-high-performance liquid chromatography (UPLC) [3, 48], the measured features would be dominated by the shape of the response function itself (Eq. 1).

Flow through pipes [49] and chromatography [50] under isocratic conditions are described by the classic Hagen–Poiseuille model of laminar flow (Fig. 3a). By adding diffusion to the Hagen–Poiseuille model with equal upstream and downstream diffusion rates, a Gaussian-shaped peak is expected [19] (Fig. 3b). Within the context of the present model, none of these flow patterns corresponded to observations where, first and foremost, the distribution of solute molecules was not symmetric around the mid-point of the pulse (see Sect. 3.4 below). Second, the time of maximum response corresponded to the time of pulse exit, whereas the middle of the pulse would be expected to be associated with the peak maximum.

Chemical species interact with column materials by means of adsorption, which removes chemicals from front of the pulse and shifts them towards the rear of the pulse (Fig. 3c) whilst the pulse travels downstream within the tubular system. Then, the diffusion term of the Navier–Stokes equation pertaining to flow through pipes becomes insignificant [10], and the term of radial transport may become non-zero [51].

3.3 Impurities and system peaks

The injection process may form minor peaks in the chromatogram that have nothing to do with the solute, but it may provide information about the dynamics of chromatographic elution. Previously, these peaks have been denoted as ghost peaks [52], peaks of impurities [53] or system peaks [54]. A tiny leading peak that originates from the injection process arrives at the detector first at time *t*(1) (Fig. 4a), and it is proposed that it arrives faster in the detector owing to the faster eluent LFR along the centreline of the pipe, according to the mechanism of laminar flow (Fig. 3a) [19, 50]. However, the diameter of the path through the column is not uniform, so it is expected that

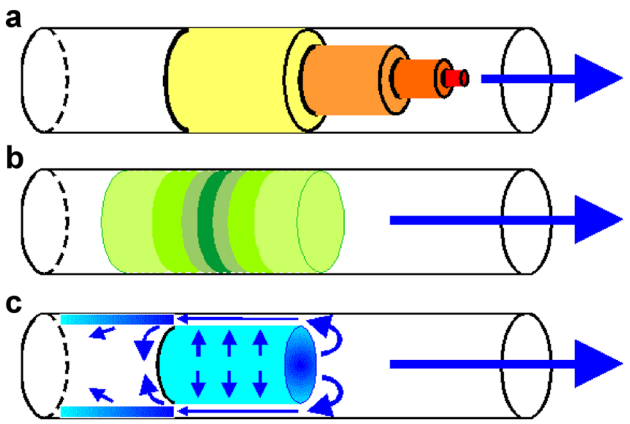

Fig. 3 Schematic illustration of flow patterns. The classical Hagen–Poiseuille model **a** of laminar flow predicts fast transport of chemicals along the centre of the pipe, whereas plate theory suggests a Gaussian distribution of chemicals **b** that is formed by equal diffusion rates along the upstream and downstream directions of flow. The present model indicates pulse flow with transport of injected chemicals within a cylindrical volume **c** that remains slightly elongated towards the downstream direction of flow

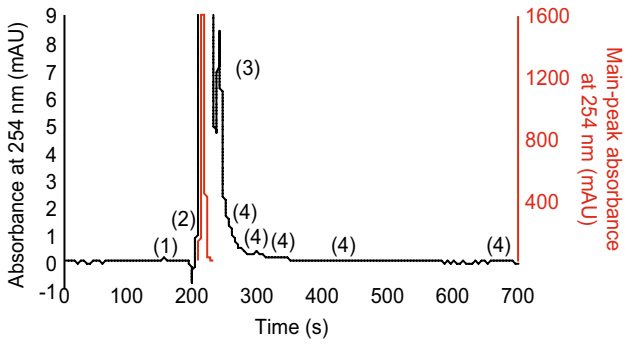

Fig. 4 Main peak (red) and subsidiary peaks (black) at a linear flow rate of 0.22 m s^{-1}. The peak heights of minor peaks (black) may be up to three orders of magnitude lower than that of the main peak (red). A small leading peak (1) created by disturbance of the injection valve was found at the front of the main peak, together with mixing peaks (2) and (3), closer to the main peak, which are formed upon injection by chemicals or air mixing with carrier solvents. Tentatively, peaks (4) in the wake of the injected pulse may be formed by the release of chemicals from the column material to the solvent of the eluent

the time of travel of the centreline peak ($t(1)$) is not precisely twice as fast as the average LFR, which otherwise characterises laminar-Hagen–Poiseuille flow through pipes.

Since the time of the pulse leaving the detection cell corresponded to the time given by Eq. 4, it may also be that the pulse expands slightly in the forward direction of flow (downstream). Minor peaks along the tail of the main peak (Fig. 4d) may be attributed to either impurities or to loss of solute from the walls after adsorption [52, 53].

The unexpected long distance of flow of the pulse may be explained by the mechanism of flow through a column, which is portrayed in Fig. 2. Tentatively, as the pulse enters the column, it finds its way through the column along void volumes that are created between grains of column material. It may even be possible that the pulse travels forth and back with respect to the direction of the overall flow rate of the chromatographic band (Fig. 2). Thus, the pulse wriggles its way through the column through an optimal pathway that is of non-uniform diameter and much longer than the length of the column. Accordingly, the apparent distribution of chemicals along the length of the column may be Gaussian shaped, whereas the concentration of chemicals along the length of the pulse itself remains virtually constant. The distribution of chemicals along the length of the column constitutes the concentration profile that is usually denoted as the 'chromatographic band' of chemicals moving through the column at a velocity, v_B, that is given by approx. $v_B \sim L/t_R$, or much slower than the LFR. Thus, the band velocities ranged from approximately 2.3×10^{-5} m s^{-1} to 0.011 m s^{-1}. Tentatively, flow dynamics of column chromatography would be characterised by a band velocity where diffusion and equilibria would generate a Gaussian-shaped band that could be described by plate theory. Then, the difference between the present description and that of plate theory would simply be related to the rate at which the pulse passes grains of the column material.

3.4 Band-broadening and peak asymmetry

At the front of the chromatographic peak, the time of half peak height is denoted as t_- and the corresponding time of half peak height along the tail is denoted as t_+. Accordingly, the *FWHM* is given by the difference $FWHM = t_+ - t_-$. A combination of Eqs. 2a–2d and Eq. 3 thus leads to the following expressions for the differences in time between time of peak maximum (t_{max}, Eq. 3) and those two points in time:

$$t_+ - t_{max} = -\frac{L_c}{v_x} \cdot ln\left(1 - \sqrt{\frac{1}{2}}\right) \tag{5a}$$

$$t_{max} - t_- = t_1 - t_0 + \frac{L_c}{v_x} \cdot ln\left[\left(1 + \frac{p}{q}\right) \cdot \left(1 - \sqrt{\frac{1 - \frac{p}{q}}{2 \cdot \left(1 + \frac{p}{q}\right)}}\right)\right] \tag{5b}$$

The ratio of p/q increases as a function of LFR, and at slow LFRs, the ratio of p/q is small, which leads to the approximation: $t_1 - t_0 \cong t_+ - t_- = FWHM$. That is, the core of the pulse, that is represented by t_1–t_0, is also found to approximately representing the FWHM, which supports the notion that the flow being of laminar type [19]. However, the laminar structure cannot be identified at slow LFRs because there is the dispersion dominated by diffusion. Therefore, Eqs. 5a and 5b are not valid at slow LFRs. Since the two differences of points in time (Eqs. 5a and 5b) are not similar, they may be used to estimate the peak asymmetry that characterises the peak in the absence of diffusion. Further, it may be shown that t_- and t_+ depend almost linearly upon t_{max} (Eq. 3) (not shown), in accord with findings of Baeza–Baeza et al. [55]. Since the separation between right-half-peak width (Eq. 5a) and left-half-peak width (Eq. 5b) is very sensitive to solvent composition of the mobile phase and to choice of column [55], it is thus suggested that the parameter L_c is important to the investigation of those features of chromatographic elution. Although the definitions are different between the present work and that of Farnan et al. [56] the symbol of 'χ' may be used to calculate the ratio of Eqs. 5a and 5b, which is the asymmetry factor representing peak skewness, as follows:

$$\chi = \frac{t_+ - t_{max}}{t_{max} - t_-} \tag{6}$$

Experimentally, this ratio was found to be larger than 1 but the theory predicted values that are lower by approx. 20%, as portrayed in Fig. 6. The difference between theory and experiment may be attributed to experimental uncertainty. The theory predicts very small asymmetry factors at slow LFRs, which characterises the flow under conditions of without diffusion. The theory is qualitatively correct in the sense that the peak asymmetry increases as a function of LFR at medium-fast LFRs that are the conditions that are most frequently used in experiments of HPLC. According to theory, the asymmetry decreases at faster LFRs, but the large scattering of experimental data does not allow for a firm confirmation of that trend, however (Fig. 5). It was thus indicated that the optimum conditions of chromatographic separation occur where both peak height and peak asymmetry are high. A higher degree of peak symmetry may be found with faster LFRs that are used for experiments of UPLC, and this may lead to comparison with Gaussian functions under such conditions of fast flow.

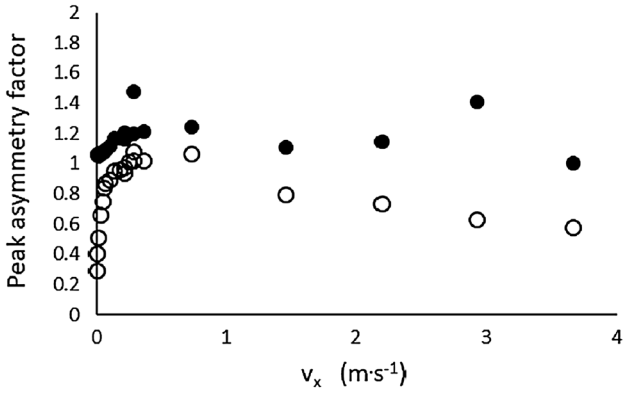

Fig. 5 Broadening of peaks, as represented by the asymmetry factor (χ) of Eq. 6, depicted as a function of LFR (v_x). The experiments (filled circle) show that the peaks are symmetric at slow LFRs, but asymmetry increases as a function of LFR until maximum asymmetry was achieved at an LFR that corresponds to the transition from pure pulse flow to flow that is influenced by packing of the column. The theory to Eq. 6 (empty circle) provided values that were lower than the experimental values by approx. 20% at medium to fast LFRs. However, with slow LFRs, the theory corresponds not to the experiment because the theory (empty circle) does not consider the influence of diffusion on the broadening of the peak

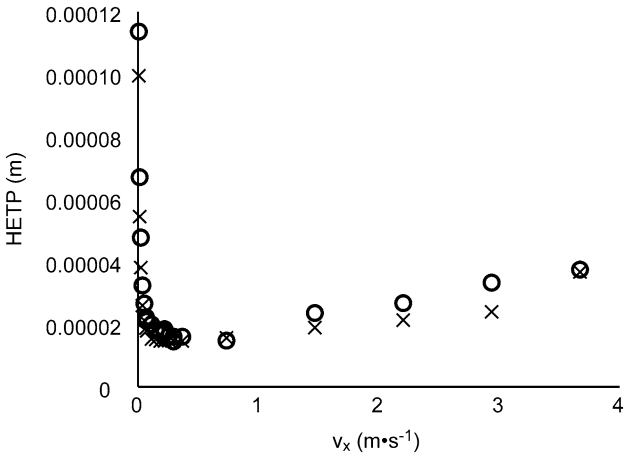

Fig. 6 Explanation of the van Deemter equation. The depiction of theoretical values of *HETP* (Eq. 8, empty circle) as a function of linear flow rate (v_x) corresponds well to experimental values (×). The minimum *HETP* is explained as the flow rate where the response time of the detector (t_D) was comparable to t_1–t_0; that is, $t_D \sim t_1$–t_0 (see text). At even faster linear flow rates, the effects of column packing add to the increasing trend of *HETP* versus v_x

3.5 The van Deemter equation

Conventionally, column properties may be described in terms of plate theory, which describes the peak shape and resolution of chromatographic systems [23, 34]. A narrow peak is desirable in chromatography as it indicates good resolution and high sensitivity [5, 14, 18]. Thus, the length of the column, L, is divided by the number of theoretical plates of the column, which gives the height equivalent to the theoretical plate (*HETP*) [23, 57] according to Eq. 7:

$$HETP = \frac{L}{5.55} \cdot \left(\frac{FWHM}{t_R}\right)^2 \tag{7}$$

The retention time corresponds to the time of peak maximum (Eq. 3). By introducing valid approximations, such as $FWHM \cong t_1 - t_0$ and $t_1 \cong t_R$, Eq. 7 simplifies to the following equation:

$$HETP = \frac{L}{5.55} \cdot \left(1 - \frac{t_0}{t_1}\right)^2 \tag{8}$$

Hence, the HETP of Eq. 8 may be depicted as a function of LFR, which provides a straightforward explanation for the van Deemter equation [23] in chromatography (Fig. 6). Thus, the ratio of t_0/t_1 was found to be not constant, which shows that the pulse velocity at the entrance to the detector was slightly different from the velocity at the exit from the detector. Therefore, the best resolution of the chromatographic system [57] was obtained at the LFR where the time of pulse passage through the detector became so short that it started to become influenced by the response time of the detector and packing of the column during each elution [29, 58].

Since the time difference of t_1–t_0 corresponded well to the FWHM, the idea of laminar structure (Fig. 3a) would be supported. However, transport of solute molecules from front to rear part of the pulse would alter this image slightly and produce a pulse with tail, as portrayed in Fig. 3c.

3.6 Peak areas

To further consolidate this notion of pulse flow and the overall model predictions, the peak area was also estimated. By integrating the convoluted peaks (Eqs. 2a–2d), it was found that the observed peak area of the pulse, that is, the convoluted area between t_0 and t_1, may be approximated by the expression:

$$A_1 \cong \frac{H \cdot L_c^2}{4 \cdot v_x} \cdot \left(\left(\frac{p}{q} - 2\right)^2 - 1\right) \tag{9}$$

This area (Eq. 9) corresponded to the area of the pulse passing through the detector without dissolution by carrier solution during flow. That is, a good correspondence was found between A_1 (Eq. 9) and the corresponding area, $A_{plug} = P_0 \cdot \frac{L_0}{v_x}$, where P_0 is the convoluted peak value that corresponds to the concentration of solute molecules in the pulse before injection. Finally, the full area of the

chromatographic peak may be calculated by the following equation (Eq. 10):

$$A = 2 \cdot A_1 - \frac{H \cdot L_c^2}{4 \cdot v_x} \tag{10}$$

Thus, the units of area are mAU s^2 after convolution, in contrast to the units of mAU s that are normally associated with peak areas in chromatography. Equation 8 shows the total area under fast transport, $A = 2 \cdot A_1$ (Eq. 10), but in contrast to the implications of the equation, the peak is not symmetric (Eqs. 2a–2d).

In many chromatographic experiments, the retention time of Eq. 3 does not strongly depend on L_c. However, the area dependence on L_c-squared (Eqs. 9, 10) shows that the value of the area is strongly influenced by both the detector and the flow dynamics. Although the length of the detection cell (0.01 m) was ignored in deriving Eqs. 2a–2d, it may be worthwhile to consider this value for the sake of understanding the influence of the detector on concentration changes, as such changes occur within the pulse during flow through the detection cell. At the fastest LFR of 3.7 m s^{-1}, the time for the signal to rise from background level to maximum absorbance would be $\Delta t = 0.01$ m/LFR of 3.7 m $s^{-1} = 0.0027$ s, which is much shorter than response time of the detector $t_D = (0.295 \pm 0.033)$ s. The corresponding filling time of the detection cell is $\Delta t = 1.37$ s at the slower flow rate of 0.0073 m s^{-1}, which, on the other hand, is much longer than t_D. At the very commonly used LFR of $v_x = 0.73$ m s^{-1} (~ 1 mL min^{-1}), the time interval to fill the cell would be $\Delta t = 0.014$ s, which, again, is much shorter than t_D. These calculations and Eqs. 9 and 10 show that both the area of and changes within the chromatographic peak are significantly influenced by the response time of the detector, as opposed to previous statements [38]. Only at slow LFRs will any change in concentration within the travelling pulse be registered in real time when those changes are slower than the time of baseline to response of the detector, which would be even longer than the t_D of approx. two times the rise time (0.88 s) when the rise time and fall time of the detector are considered equal. This value of 0.88 s shows that only very slow changes may be monitored without the influence of the detector's response function.

4 Conclusion

A simplified description based on pulse flow was presented, and it was shown that the response time of the detector should not be ignored in chromatography. Fast detector response times are required to monitor changes in the concentration of solute molecules after interactions with the column material. According to the theory of pipe laminar flow, mobile phase passes though the travelling pulse, but solute molecules interact with the column material. Tentatively, solute molecules are delayed by short-term interactions that allow the solute molecules to be released back from the column material into the travelling pulse, which is in support of the adsorption theory. The degree of interaction and time of adsorption of solute to column material thus depends on the characteristic length (L_c), which was determined as $L_c = (0.555 \pm 0.011)$ for caffeine in methanol, which interacts weakly with the C-18 column material. It was proposed that upon injection into the eluent, the pulse travels very long distances back and forth between cavities created by grains of the column material, thus creating a chromatographic band with an approximate Gaussian shape. Thus, the flow may be regarded as open-end flow involving adsorption processes but to a lesser extent involves equilibria subject to plate theory. This alternative understanding of the chromatographic process was developed by including the detector response function in the evaluation of data. By taking the simplified description further, it was also proposed that the van Deemter curve is shaped by the small difference between the flow rates at the point of entrance to the detection cell and the point of exit from the detection cell (Eq. 6). Therefore, focus should also be directed towards including detector properties to obtain a deeper understanding of flow patterns in pipe flow and chromatography.

Acknowledgments The financial support of this work by the Botswana International University of Science and Technology is gratefully acknowledged.

Author contributions HWM and IWM prepared the chemicals, performed the experiments and filed data for processing. JETA performed the data analysis, developed the theory and wrote the manuscript.

Funding Botswana International University of Science and Technology (BIUST), Department of Chemical and Forensic Sciences.

Compliance with ethical standards

Conflict of interest The authors declare that they have no conflict of interest.

Ethical approval This article does not contain any studies with human or animal subjects.

Appendix 1

See Table 1.

Table 1 Nomenclature and magnitudes of selected parameters

Parameter	Meaning
α	Experimentally determined maximum response of detector (8750 ± 610) mAU
β	Experimentally determined reciprocal time constant of detector (− 3.39 ± 0.38) s^{-1}
t_D	Experimentally determined response time of detector (0.295 ± 0.033) s
v_x	Linear flow rate (LFR) of eluent
H	Maximum response of caffeine analysis
L_c	Characteristic length of detector in combination with flow dynamics
t_0	Time of entrance to detection cell of the pulse-shaped volume containing caffeine
t_1	Time of exit from detection cell of the pulse-shaped volume containing caffeine
p	Peak-exponential function at pulse entrance to cell of detection
q	Peak-exponential function of pulse exit from cell of detection
t_{max}	Time of peak maximum
t_-	Time of half maximum, left-hand side of peak
t_+	Time of half maximum, right-hand side of peak
χ	Peak asymmetry factor
A_1	Peak area measured from t_0 to t_{max}
A_2	Peak area measured from t_{max} to infinite time
A	Total peak area determined from t_0 to infinite time
L	Length of column (0.15 m)
L(pulse)	Cylindrically shaped length of the travelling segment containing caffeine (solute) that travels within tubes and column
L_0	Length of pulse that corresponds to the volume of segment containing caffeine (solute) that was injected into 0.17 micron-bore tubes
HETP	Height equivalent to the theoretical plate in units of metres
FWHM	Full width at half maximum of the chromatographic peak. Value of time with units of seconds
$t_{(1)}$	Time of the small peak observed as a small disturbance to the baseline signal before the main peak was observed in each chromatogram

References

1. Pontrelli G (2006) The role of the arterial prestress in blood flow dynamics. Med Eng Phys 28:6–12. https://doi.org/10.1016/j.medengphy.2005.04.013
2. Asnin LD, Stepanova MV (2018) Van't Hoff analysis in chiral chromatography. J Sep Sci 41:1319–1337. https://doi.org/10.1002/jssc.201701264
3. Swartz ME (2005) UPLC™: an introduction and review. J Liq Chromatogr Relat Technol 28:1253–1263. https://doi.org/10.1081/JLC-200053046
4. Carr PW, Stoll DR, Wang X (2011) Perspectives on recent advances in the speed of high-performance liquid chromatography. Anal Chem 83:1890–1900
5. Poppe H (1997) Some reflections on speed and efficiency of modem chromatographic methods. J Chromatogr A 778:3–21
6. Grinias JP, Kennedy RT (2016) Advances in and prospects of microchip liquid chromatography. TrAC Trends Anal Chem 81:110–117. https://doi.org/10.1016/j.trac.2015.08.002
7. Grinias JP, Kennedy RT (2015) Evaluation of 5 micron superficially porous particles for capillary and microfluidic LC columns. Chromatography 2:502–514. https://doi.org/10.3390/chromatography2030502
8. Green R, Brown R, Pletcher D (2015) Understanding the performance of a microfluidic electrolysis cell for routine organic electrosynthesis. J Flow Chem 5:31–36. https://doi.org/10.1556/JFC-D-14-00027
9. Shimizu H, Smirnova A, Mawatari K, Kitamori T (2017) Extended-nano chromatography. J Chromatogr A 1490:11–20. https://doi.org/10.1016/j.chroma.2016.09.012
10. Weigl BH, Bardell RL, Cabrera CR (2003) Lab-on-a-chip for drug development. Adv Drug Deliv Rev 55:349–377. https://doi.org/10.1016/S0169-409X(02)00223-5
11. Ortner F, Ruppli C, Mazzotti M (2018) Description of adsorption in liquid chromatography under nonideal conditions. Langmuir 34:5655–5671. https://doi.org/10.1021/acs.langmuir.8b00552
12. Giddings JC, Eyring H (1955) A molecular dynamic theory of chromatography. J Phys Chem 59:416–421
13. Martin AJP, Synge RLM (1941) A new form of chromatogram employing two liquid phases 1. A theory of chromatography 2. Application to the micro-determination of the higher monoamino-acids in proteins. Biochem J 35:1358–1368
14. Lee W, Tsai G-J, Tsao GT (1993) Analysis of chromatography by plate theory. Sep Technol 3:178–197
15. Vailaya A, Horvath C (1998) Retention in reversed-phase chromatography: partition or adsorption? J Chromatogr A 829:1–27
16. Eiceman GA, Hill HH, Gardea-Torresdey J (1998) Gas chromatography. Anal Chem 70:321–339. https://doi.org/10.1021/a1980016l
17. Lian E, Ren Y, Han Y et al (2016) Multi-scale morphological analysis of conductance signals in vertical upward gas-liquid two-phase flow. Z Naturforsch Sect A J Phys Sci 71:1031–1052. https://doi.org/10.1515/zna-2016-0235

18. Swartz M (2010) HPLC detectors: a brief review. J Liq Chromatogr Relat Technol 33:1130–1150. https://doi.org/10.1080/10826076.2010.484356
19. Taylor G (1953) Dispersion of soluble matter in solvent flowing slowly through a tube. R Soc Chem 219:186–203
20. Appleton JMH, Tyson J (1986) Flow injection atomic absorption spectrometry: the kinetics of instrument response. J Anal At Spectrom 1:63–74
21. Butler C, Lalanne B, Sandmann K et al (2018) Mass transfer in Taylor flow: transfer rate modelling from measurements at the slug and film scale. Int J Multiph Flow 105:185–201. https://doi.org/10.1016/j.ijmultiphaseflow.2018.04.005
22. Silva MR, Andrade FN, Fumes BH, Lanças FM (2015) Unified chromatography: fundamentals, instrumentation and applications. J Sep Sci 38:3071–3083. https://doi.org/10.1002/jssc.201500130
23. van Deemter JJ, Zuiderweg FJ, Klinkenberg A (1956) Longitudinal diffussion and resistance to mass transfer as causes of nonideality in chromatography. Chem Eng Sci 5:271–289
24. Pápai Z, Pap TL (2002) Analysis of peak asymmetry in chromatography. J Chromatogr A 953:31–38. https://doi.org/10.1016/S0021-9673(02)00121-8
25. Beisler AT, Schaefer KE, Weber SG (2003) Simple method for the quantitative examination of extra column band broadening in microchromatographic systems. J Chromatogr A 986:247–251. https://doi.org/10.1016/S0021-9673(02)02018-6
26. Schiel JE, Ohnmacht CM, Hage DS (2009) Measurement of drug-protein dissociation rates by high-performance affinity chromatography and peak profiling. Anal Chem 81:4320–4333. https://doi.org/10.1021/ac9000404
27. Li J, Carr PW (1997) Evaluation of temperature effects on selectivity in RPLC separations using polybutadiene-coated zirconia. Anal Chem 69:2202–2206. https://doi.org/10.1021/ac9608681
28. Miyabe K (2016) Moment theory for kinetic study of chromatography. TrAC Trends Anal Chem 81:79–86. https://doi.org/10.1016/j.trac.2016.01.003
29. Blue LE, Jorgenson JW (2015) 1. 1 µm superficially porous particles for liquid chromatography Part II: column packing and chromatographic performance. J Chromatogr A 1380:71–80. https://doi.org/10.1016/j.chroma.2014.12.055
30. Ye C, Terfloth G, Li Y, Kord A (2009) A systematic stability evaluation of analytical RP-HPLC columns. J Pharm Biomed Anal 50:426–431. https://doi.org/10.1016/j.jpba.2009.05.028
31. Jandera P, Sromová Z (2018) Mobile phase effects in reversed-phase and hydrophilic interaction liquid chromatography revisited. J Chromatogr A 1543:48–57. https://doi.org/10.1016/j.chroma.2018.02.043
32. Han SY, Qiao JQ, Zhang YY et al (2012) Determination of n-octanol/water partition coefficients of weak ionizable solutes by RP-HPLC with neutral model compounds. Talanta 97:355–361. https://doi.org/10.1016/j.talanta.2012.04.045
33. De Pauw R, Choikhet K, Desmet G, Broeckhoven K (2014) Occurrence of turbulent flow conditions in supercritical fluid chromatography. J Chromatogr A 1361:277–285. https://doi.org/10.1016/j.chroma.2014.07.088
34. Nesterenko PN, Rybalko A, Paull B (2005) Significant viscosity dependent deviations from classical van Deemter theory in liquid chromatography with porous silica monolithic columns. Analyst 130:828–830. https://doi.org/10.1039/b502514a
35. Vanderheyden Y, Broeckhoven K, Desmet G (2016) Peak deconvolution to correctly assess the band broadening of chromatographic columns. J Chromatogr A 1465:126–142. https://doi.org/10.1016/j.chroma.2016.08.058
36. Wright NA, Villalanti DC, Burke MF (1982) Fourier transform deconvolution of instrument and column band broadening in liquid chromatography. Anal Chem 54:1735–1738. https://doi.org/10.1021/ac00248a019
37. Andersen JET (2000) Indications of segmental flow in straight pipes by flow injection with spectrophotometric detection. Phys Scr 62:331–340. https://doi.org/10.1238/Physica.Regular.062a00331
38. Wahab MF, Dasgupta PK, Kadjo AF, Armstrong DW (2016) Sampling frequency, response times and embedded signal filtration in fast, high efficiency liquid chromatography: a tutorial. Anal Chim Acta 907:31–44. https://doi.org/10.1016/j.aca.2015.11.043
39. Felinger A, Kilár A, Boros B (2015) The myth of data acquisition rate. Anal Chim Acta 854:178–182. https://doi.org/10.1016/j.aca.2014.11.014
40. Vanderheyden Y, Vanderlinden K, Broeckhoven K, Desmet G (2016) Problems involving the determination of the column-only band broadening in columns producing narrow and tailed peaks. J Chromatogr A 1440:74–84. https://doi.org/10.1016/j.chroma.2016.02.042
41. Pap TL, Pápai Z (2001) Application of a new mathematical function for describing chromatographic peaks. J Chromatogr A 930:53–60
42. Hatrík Š, Hrouzek J (1994) The use of general exponential function for the deconvolution of fused chromatographic peaks. Chem Pap 48:376–380
43. Andersen JET (2001) On the possibility to improve the performance of flow injection analysis by deconvolution of spectrophotometric data. Talanta 54:131–138. https://doi.org/10.1016/S0039-9140(00)00642-1
44. Draper JW III, Lee SW, Marineau EC (2018) Numerical construction of impulse response functions and input signal reconstruction. J Sound Vib 432:259–271. https://doi.org/10.1016/j.jsv.2018.06.041
45. Katz E, Ogan KL, Scott RPW (1983) Peak dispersion and mobile phase velocity in liquid chromatography: the pertinent relationship for porous silica. J Chromatogr 270:51–75. https://doi.org/10.1016/S0021-9673(01)96351-4
46. Augustin V, Jardy A, Gareil P, Hennion MC (2006) In situ synthesis of monolithic stationary phases for electrochromatographic separations: study of polymerization conditions. J Chromatogr A 1119:80–87. https://doi.org/10.1016/j.chroma.2006.02.057
47. Andersen JET (2010) Novel response function resolves by image deconvolution more details of surface nanomorphology. Phys Scr 82:055602. https://doi.org/10.1088/0031-8949/82/05/055602
48. Walter TH, Andrews RW (2014) Recent innovations in UHPLC columns and instrumentation. Trends Anal Chem 63:14–20. https://doi.org/10.1016/j.trac.2014.07.016
49. Striegel AM (2016) Viscometric detection in size-exclusion chromatography: principles and select applications. Chromatographia 79:945–960. https://doi.org/10.1007/s10337-016-3078-0
50. Chester TL (2013) Recent developments in high-performance liquid chromatography stationary phases. Anal Chem 85:579–589
51. Gritti F (2018) On the relationship between radial structure heterogeneities and efficiency of chromatographic columns. J Chromatogr A 1533:112–126. https://doi.org/10.1016/j.chroma.2017.12.030
52. Williams S (2004) Ghost peaks in reversed-phase gradient HPLC: a review and update. J Chromatogr A 1052:1–11. https://doi.org/10.1016/j.chroma.2004.07.110
53. Jin J, Wang Z, Lin J et al (2017) Journal of pharmaceutical and biomedical analysis "Ghost peaks" of ezetimibe: solution degradation products of ezetimibe in acetonitrile induced by alkaline impurities from glass HPLC vials. J Pharm Biomed Anal 140:281–286. https://doi.org/10.1016/j.jpba.2017.02.059

54. Levin S, Grushka E (1986) System peaks in liquid chromatography: their origin, formation, and importance. Anal Chem 58:1602–1607
55. Baeza-Baeza JJ, Pous-Torres S, Torres-Lapasió JR, García-Álvarez-Coque MC (2010) Approaches to characterise chromatographic column performance based on global parameters accounting for peak broadening and skewness. J Chromatogr A 1217:2147–2157. https://doi.org/10.1016/j.chroma.2010.02.010
56. Farnan D, Frey DD, Horváth C (1997) Intraparticle mass transfer in high-speed chromatography of proteins. Biotechnol Prog 13:429–439. https://doi.org/10.1021/bp970044k
57. Carr PW, Wang X, Stoll DR (2009) Effect of pressure, particle size, and time on optimizing performance in liquid chromatography. Anal Chem 81:5342–5353. https://doi.org/10.1021/ac9001244
58. Liekens A, Billen J, Sherant R et al (2011) High performance liquid chromatography column packings with deliberately broadened particle size distribution: relation between column performance and packing structure. J Chromatogr A 1218:6654–6662. https://doi.org/10.1016/j.chroma.2011.07.055